Biochemistry

Article

pubs.acs.org/biochemistry

# Chemical Denaturants Smoothen Ruggedness on the Free Energy Landscape of Protein Folding

Pooja Malhotra, Prashant N. Jethva, and Jayant B. Udgaonkar*

National Centre for Biological Sciences, Tata Institute of Fundamental Research, Bengaluru 560065, India

Supporting Information

**ABSTRACT:** To characterize experimentally the ruggedness of the free energy landscape of protein folding is challenging, because the distributed small free energy barriers are usually dominated by one, or a few, large activation free energy barriers. This study delineates changes in the roughness of the free energy landscape by making use of the observation that a decrease in ruggedness is accompanied invariably by an increase in folding cooperativity. Hydrogen exchange (HX) coupled to mass spectrometry was used to detect transient sampling of local energy minima and the global unfolded state on the free energy landscape of the small protein single-chain monellin. Under native conditions, local noncooperative openings result in interconversions between Boltzmann-distributed intermediate states, populated on an extremely rugged "uphill" energy landscape. The cooperativity of these interconversions was increased by selectively destabilizing the native state via mutations, and further by the addition of a chemical denaturant. The perturbation of stability alone resulted in seven backbone amide sites exchanging cooperatively. The size of the cooperatively exchanging and/or unfolding unit did not depend on the extent of protein destabilization. Only upon the addition of a denaturant to a destabilized mutant variant did seven additional backbone amide sites exchange cooperatively. Segmentwise analysis of the HX kinetics of the mutant variants further confirmed that the observed increase in cooperativity was due to the smoothing of the ruggedness of the free energy landscape of folding of the protein by the chemical denaturant.

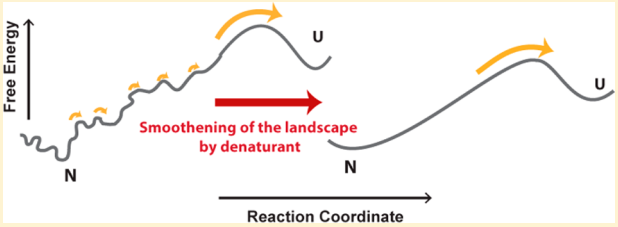


The free energy landscape accessible to a folded protein is riddled with a multitude of high-energy conformations, populated according to their Boltzmann distributions.[1,2] Some of these higher-energy conformations are obligatory and play productive roles in the folding and unfolding pathways.[3−7] Other conformations may be kinetic traps that slow folding,[8−10] because they possess physicochemical interactions that are inconsistent with each other.[11] In particular, non-native interactions[12] can lead to "frustration".[13] The presence of productive intermediates as well as frustrated conformations is a characteristic feature of a rugged free energy landscape of folding. Delineating the presence of high-energy conformations that define the ruggedness of the landscape has, however, been experimentally challenging, because the small (∼2−3 $k_BT$) free energy barriers that separate them are usually dominated by one, or a few, large barriers.

Experimental probes that are used to monitor protein folding and unfolding reactions are sensitive principally to the larger free energy barriers on the landscape and are, therefore, unable to detect sparsely populated conformations separated by small free energy barriers, which arise because of small local mismatches in enthalpy−entropy changes.[13,14] One strategy that has been applied to circumvent this difficulty is to characterize the energy landscape of downhill folding proteins.[15−20] The rapid folding of these proteins has been shown to be slowed by an inherently rough energy landscape, even in the absence of a significant energy barrier.[17] More direct attempts to delineate experimentally the roughness of the free energy landscape of protein folding include the determination of internal friction[21−26] as well as transition path times.[27−29]

Changes in the cooperativity of a folding−unfolding reaction provide another means of probing the ruggedness of the free energy landscape of folding. A fully cooperative folding−unfolding transition involves the population of only the native (N) and unfolded (U) states, separated by a single activation energy barrier. At the other extreme is a fully noncooperative gradual transition, which involves the population of a continuum of intermediate states between N and U, separated by many small energy barriers. For a typical protein, the N and U states are, however, separated by many small free energy barriers as well as one, or a few, large free energy barriers. A reduction in the number of free energy barriers, i.e., a smoothing of roughness on the free energy landscape of protein folding, would therefore increase the cooperativity of a folding−unfolding reaction.

The work presented here explores a novel strategy for delineating directly the smoothing of a rough free energy landscape, using changes in the cooperativity of a gradual "uphill" unfolding reaction as a measurable parameter. Cooperativity can be affected by changes in experimental conditions that perturb the thermodynamic stabilities of the N and U states and modulate the energy bias toward N or U.[30,31] Folding

**Received:** April 21, 2017
**Revised:** July 10, 2017
**Published:** July 17, 2017





DOI: 10.1021/acs.biochem.7b00367
*Biochemistry* 2017, 56, 4053−4063

cooperativity can thus be tuned between the two extremes of a two-state and a gradual transition, as shown in Figure 1. In the

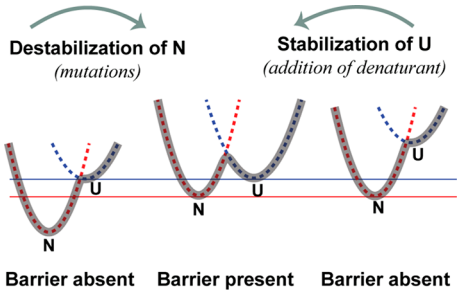


**Figure 1.** Tuning protein folding cooperativity by modulating stability. The N (red) and U (blue) state energy wells, as well as the resultant free energy surface (gray), are shown for a barrier-less and a barrier-limited transition. The point of intersection of the N and U energy wells represents the transition state (TS) of the reaction. When the TS and U states are at similar energy levels, the activation free energy barrier to unfolding disappears (left and right panels). Mutations that destabilize the N state, or changes in solution conditions that preferentially stabilize the U state, can result in a barrier-limited unfolding transition (middle panel), as described in the text. Modified and reproduced with permission from ref 41.

study presented here, the cooperativity of an unfolding reaction has been tuned in two different ways: (1) by selectively destabilizing the N state via site-specific mutations and (2) by adding a chemical denaturant that preferentially stabilizes the U state. A comparison of the changes in cooperativity induced by these two methods has shown that changes in cooperativity can be used to demonstrate the smoothing of a rough free energy landscape. An important inference that has emerged from these observations is that the conditions under which many folding and unfolding studies are carried out may modulate the inherent ruggedness of the free energy landscape of protein folding and may thus themselves alter the folding mechanism.

Hydrogen exchange coupled to mass spectrometry (HX−MS) experiments with the protein single-chain monellin (MNEI)[31,32] have provided a good example of an "uphill" unfolding reaction that occurs over an extremely rough free energy landscape. Under native conditions, all the backbone amide sites of the protein lost structure one at a time, in a gradual manner. The transient sampling of the U state under native conditions occurred in a barrier-less manner, via a multitude of conformations separated by small free energy barriers. The addition of a chemical denaturant, guanidine hydrochloride (GdnHCl), which preferentially stabilized the U state, caused a subset of the backbone amide sites, involved in the global unfolding transition, to open in a concerted manner. Hence, as shown in Figure 1, changes in the stability of the U state induced cooperativity in the global unfolding transition.

In the study presented here, the cooperativity of the unfolding reaction has been monitored by HX−MS for mutant variants of MNEI. Selective destabilization of the N state, via mutations, induced cooperative unfolding of seven backbone amide sites. This provides a measure of the extent of cooperativity that can be induced by changes in the inherent thermodynamic stabilities alone. The addition of denaturant to a destabilized mutant variant caused an additional seven backbone amide sites to exchange in a concerted manner, indicating that the effect of the denaturant on the cooperativity of the transition is not solely caused by the perturbation of the apparent thermodynamic stability, as previously thought. Further analysis of the HX−MS patterns of individual sequence segments of the mutant variants confirmed that the observed increase in folding cooperativity upon the addition of a denaturant was due to the smoothing of intervening local barriers on the rough energy landscape of MNEI.

## MATERIALS AND METHODS

**Protein Purification.** Wild type (wt) and mutant variants of MNEI were purified according to the protocol described previously.[33] All mutations were made on the C42A pseudo wt construct, by site-directed mutagenesis. Protein purity was checked by mass spectrometry, and the protein concentration was measured using a molar extinction coefficient of 14600 $M^{-1}$ $cm^{-1}$.[33]

**Reagents.** All reagents used were of the highest purity grade from Sigma-Aldrich. GdnHCl of the highest purity grade was obtained from United States Biochemicals. All experiments were carried out at pH 8 and 25 °C.

**Fluorescence-Monitored Equilibrium Unfolding Transitions.** The thermodynamic stability of each protein was determined by fluorescence measurements on the MOS 450 optical system from Biologic, using an excitation wavelength of 280 nm, and collecting emission at 340 nm, using a 10 nm band-pass filter (Asahi Spectra). The final protein concentration used was 10 $\mu$M.

**Deuteration of MNEI.** Mutant and wt proteins were deuterated as described previously.[31] Briefly, 200 $\mu$M protein (in 10 mM Tris-$D_2O$ buffer) was exposed to a high pH of 12.8, which resulted in unfolding of the protein and facilitated deuteration of all exchangeable hydrogens. After 5 min, the pH was reduced to 1.6 and then gradually adjusted to 8. DCl and NaOD (1 N each) were used for pH adjustments. The fully deuterated protein retained 190 ± 2 deuteriums, for all the variants of MNEI.

**Hydrogen Exchange Kinetics.** For experiments with the intact protein, 200 $\mu$M fully deuterated protein was diluted 20-fold into protonated exchange buffer (20 mM Tris in $H_2O$) (DHX reaction). For fragmentation by electron transfer dissociation (ETD), 500 $\mu$M protein was diluted 15-fold into the exchange buffer. After different time periods, the reaction was quenched, by mixing 125 $\mu$L of the exchange reaction mixture with 375 $\mu$L of the quench buffer [100 mM glycine hydrochloride and 8 M GdnHCl (pH 2.2)] on ice, and the deuterium retention was measured as a function of time. The final quenched solution consisted of 2.5 $\mu$M protein, 75 $\mu$M glycine HCl, and 6 M GdnHCl, at pH 2.6 on ice. For L33A MNEI and C42A MNEI, protiated protein was diluted into deuterated exchange buffer (20 mM Tris in $D_2O$), and deuterium incorporation was measured after different periods of HDX. The pH values reported for $D_2O$-containing buffers were not corrected for any isotope effect. All proteins were incubated in 6 M GdnHCl for 1 min, under quenched conditions, to enhance subsequent fragmentation by ETD.[31] For exchange in the presence of a denaturant, the GdnHCl concentrations in the exchange and quench buffers were adjusted accordingly.

**Mass Spectrometric Analysis of HX Reactions.** The quenched reaction mixtures were desalted on a Sephadex G-25 Hitrap column (GE Healthcare) using an ÄKTA basic HPLC system and eluted out in Milli-Q water, at pH 2.6, on ice. The desalted samples were injected into the HDX module (Waters Corp.) of a nanoACQUITY UPLC system coupled to the Synapt G2 HD mass spectrometer. Further desalting was achieved by


DOI: 10.1021/acs.biochem.7b00367
Biochemistry 2017, 56, 4053−4063

loading the sample onto a C18 reverse phase trap column for 1 min. The protein was eluted from the trap column using a gradient from 35 to 95% acetonitrile in 3 min. The chromatography was carried out at 4 °C to minimize back exchange into the samples. The following source parameters were used for ionization: capillary voltage, 3 kV; source temperature, 80 °C; desolvation temperature, 200 °C. The instrument parameters used for ETD are described in SI Methods of the Supporting Information.

**Data Analysis.** A cumulative ion count of $>10^6$ was achieved by combining 40 scans. The resulting spectra were background-subtracted and smoothed using MassLynx version 4.1. The smoothed mass distribution of the +13 charge state was fit to a unimodal or bimodal Gaussian function in Origin. Mass distributions plotted at each time point of exchange were normalized to the total area under the curve. The shift in the centroid of the mass distribution with time of exchange was quantified as the deuterium retention/incorporation with respect to time and fitted to a sum of multiple exponentials using the Sigmaplot software. The time course of the increase in area under the mass distribution corresponding to that of the U state was fitted to a single-exponential equation to yield the apparent rate constant of formation of the U state. Data analysis of the ETD fragments has been detailed in SI Methods of the Supporting Information.

## RESULTS

**Perturbation of Global Stability via Mutations.** Figure 2A shows the locations of the amino acid residues that were

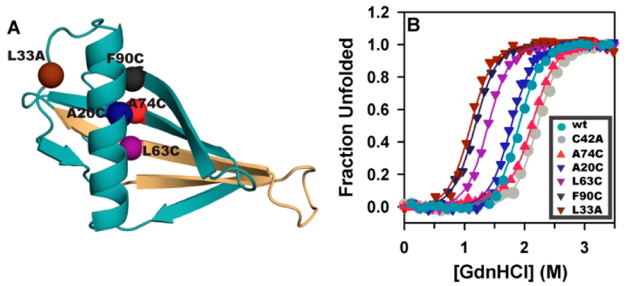


**Figure 2.** Mutant variants of MNEI that selectively destabilize the N state. (A) Structure of MNEI (Protein Data Bank entry 1IV7) showing the residues (as spheres) that were mutated one at a time on the cysteine-free pseudo wt background (C42A). $\beta$2 and $\beta$3, which contain the 14 backbone amide sites found to exchange cooperatively upon the addition of denaturant,[31] are colored light brown. (B) The fluorescence-monitored equilibrium unfolding transition of each mutant variant of MNEI was used to determine thermodynamic parameters describing unfolding at 25 °C and pH 8, as reported in Table S1.

mutated to perturb the global stability of MNEI. The mutations span each secondary structural element in the protein, including the sole $\alpha$ helix (A20C), the $\beta$ strands (L63C in $\beta$3, A74C in $\beta$4, and F90C in $\beta$5), and a loop (L33A). In most cases, completely buried residues in the protein were mutated to residues with shorter side chains, which is likely to result in cavities and, thereby, in the destabilization of the N state. The equilibrium unfolding transitions for all the mutant variants of MNEI fit well to a two-state N ↔ U model.[34] The free energy difference between N and U ($\Delta G_u$), the denaturant dependence of $\Delta G_u$ ($m$ value), and the midpoint of the denaturant-induced unfolding transition ($C_m$), obtained from the two-state fits, are listed in Table S1 for each mutant variant. The values of $\Delta G_u$ (6.3 kcal mol$^{-1}$), $m$ (−3.2 kcal mol$^{-1}$ M$^{-1}$), and $C_m$ (1.95 M) obtained for the wt protein agreed well with previously reported values at pH 8.[7,35] For all the mutant variants, except L33A MNEI, the $m$ values were found to be similar to the $m$ value measured for the wt protein. It is evident from the $\Delta G_u$ values that while the stability of A74C MNEI was similar to that of the wt protein, all other mutant variants studied here were destabilized by 0.7−2.5 kcal mol$^{-1}$ compared to wt MNEI. A20C MNEI was perturbed the least, compared to the wt protein, while maximal destabilization was observed for F90C MNEI. It should be noted here that only the destabilization of L63C, F90C, and L33A is likely to be due to the creation of a cavity.

The pseudo-wt protein (C42A MNEI) was observed to be slightly more stable than wt MNEI (by 0.5 kcal/mol) (Table S1), despite the fact that a larger cysteine side chain was replaced by a smaller alanine side chain. However, the increase in stability was small, indicating that the destabilization of A20C MNEI, L63C MNEI, F90C MNEI, and L33A MNEI was caused by the additional destabilizing mutations, and not by the C42A mutation. Nevertheless, the kinetics of HDX into C42A MNEI was measured, to ensure that the slight increase in stability did not result in a significant change in the HX behavior of the protein.

**Exchange Occurs in the EX1 Limit in wt MNEI.** Cooperative and noncooperative opening events can be distinguished directly from the observed mass distributions in HX−MS experiments only in the EX1 limit of exchange[36] (see SI Text of the Supporting Information). To infer the cooperativity of opening transitions in MNEI, it was therefore very important to determine the exchange regime for both the wt and the destabilized mutant variants, under the current experimental conditions. The fluorescence-monitored refolding rate constants of MNEI[7] were slow enough to suggest that HX into the protein would occur in the EX1 regime at pH 8. This was confirmed by measuring the pH dependence of HX rate constants.

A lack of dependence of observed HX rate constants on the pH of the solution is the most definitive test for exchange occurring in the EX1 limit. The HX kinetics of the intact protein was, indeed, similar at pH 7 and 8.[31] The measured HX rate constants for the intact protein were, however, a mean value averaged over multiple backbone amide sites that might have obscured differences in the exchange mechanisms of individual backbone amide sites. While it is very difficult to achieve single-amino acid resolution in mass spectrometry studies, individual sequence segments of the protein can be monitored to improve structural resolution.[32] Furthermore, in the case of MNEI, because exchange occurred in multiple kinetic phases, the effective comparison of the HX rate constants, measured at pH 7 and 8, was between the few amide sites that exchanged in each kinetic phase in each sequence segment, and not between all the sites observed in the given segment. Rigorous analysis of not only the deuterium exchange kinetics but also the peak shapes in the mass spectra of individual fragments of the protein ensured that even subtle changes in the mass distributions across the pH conditions could be detected.[32] Except for four backbone amide sites, the mass distributions as well as rate constants of exchange were similar (a <3-fold difference) at pH 7 and 8 under native conditions for a majority of the observed backbone amide hydrogens (a total of 44). Moreover, even the amplitudes of individual kinetic phases were similar at both pH values, indicating that the exchange kinetics of the same sites were being compared at pH 7 and 8. Careful analysis of the observed HX kinetics for the whole protein[31] as well as individual sequence


DOI: 10.1021/acs.biochem.7b00367
Biochemistry 2017, 56, 4053−4063

segments[32] therefore established that HX into wt MNEI indeed occurs in the EX1 regime, at pH 8 under native conditions. Thus, it was possible to determine changes in kinetic cooperativity in the unfolding transition of the protein.

**Exchange Occurs in the EX1 Limit in Mutant Variants.** Amino acid mutations in a protein can affect site-specific opening and closing rate constants and cause changes in the mechanism of HX.[37] However, folding−closing rate constants in a protein are expected to either decrease or remain unperturbed in a destabilized mutant variant. Hence, given that the wt protein exchanges in the EX1 regime (closing rate constant ≪ intrinsic exchange rate constant[38]), a further decrease in the closing rate constant would not result in a transition to the EX2 limit. Thus, it seemed valid to assume that exchange for the destabilized variants, as well as for A74C MNEI that is as stable as the wt protein, also occurs in the EX1 regime, at pH 8, in the absence of a denaturant. The cooperativity of the transient opening motions in the mutant variants could therefore be inferred directly from the HX−MS-monitored mass distributions.

**Effect of Destabilization on the Mass Distributions in HX−MS Experiments.** The mutant variants of MNEI were deuterated and allowed to undergo exchange in protonated solvent for different times, before the reaction was quenched, and the extent of exchange was determined by measuring the decrease in mass by mass spectrometry. In the case of L33A MNEI, protiated protein was allowed to undergo exchange in deuterated solvent, which resulted in an increase in mass with time of exchange. Because the observed HX for the wt and the mutant proteins under the experimental conditions of this study occurs in the EX1 limit, unimodal and bimodal mass distributions are indicative of noncooperative and cooperative opening transitions. As reported previously,[31] and shown in Figure 3 for the wt protein, unimodal mass spectra were observed at all times of exchange, in the absence of a denaturant, i.e., under native conditions. The observation of a constant width of the mass distributions with time of exchange[31] further confirmed the presence of only one population at all times of exchange. In the absence of any significant change in stability, as in the case of A74C MNEI (Figure S2), the mass distributions were similar to that of the wt protein and appeared to be unimodal at all times, until exchange was complete.

Destabilization of the protein resulted in a significant change in the observed mass spectra, as shown in Figure 3 and Figure S3. While the mass distributions continued to be unimodal for the first 180 s of exchange, significant widening of the distributions was observed at longer reaction time scales. This was indicative of the presence of more than one exchange-competent species. The spectra at long time points of exchange fit well to a sum of two Gaussian distributions from which the mass of each species was determined. Bimodal distributions for the destabilized mutant variants were indicative of cooperative exchange in which multiple backbone amide sites exchanged in a concerted manner. From the difference in mass between the two distributions, it was evident that approximately seven backbone amide sites exchanged cooperatively in all the mutant variants, under native conditions, regardless of the extent of destabilization. Because the mutations were made on a pseudo-wt (C42A) background, it was also confirmed that the mass distributions as well as the exchange kinetics of the pseudo-wt protein were similar to those of wt MNEI (Figure S2). The observed HX rate constants and amplitudes confirmed that the increased stability of the pseudo-wt protein did not result in any significant changes in the HX kinetics of MNEI (Table 1).

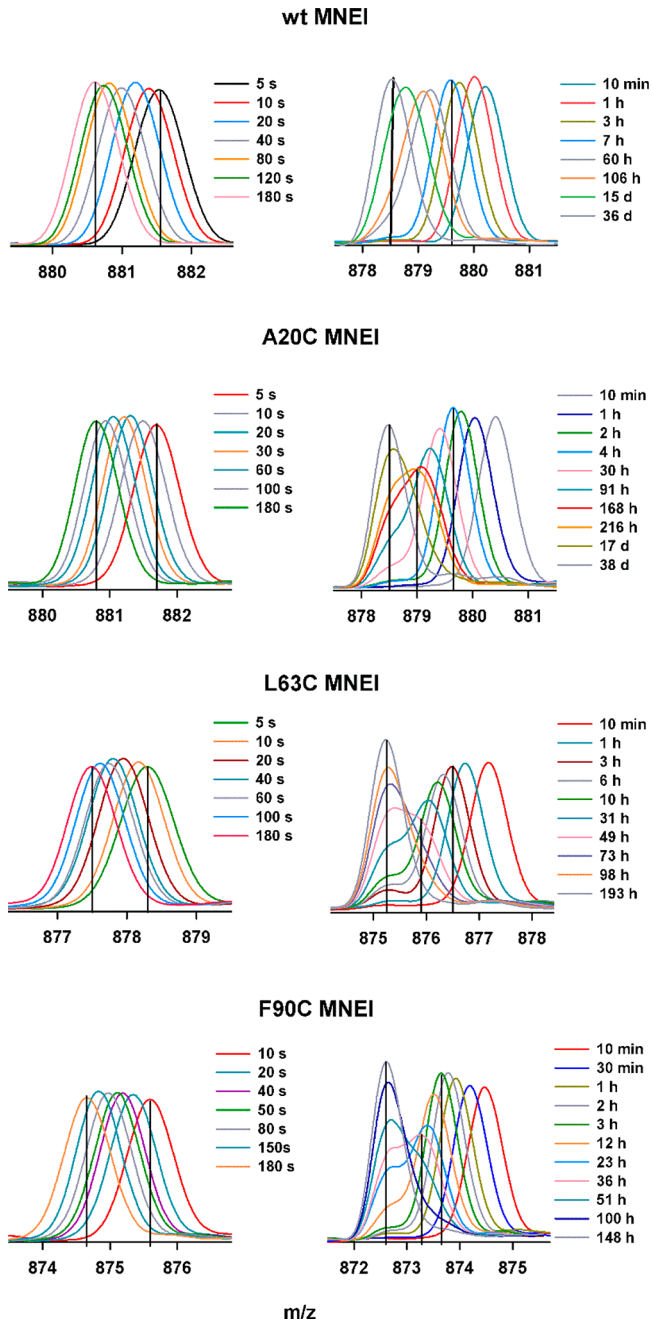


**Figure 3.** Mass distributions of destabilized MNEI variants in 0 M GdnHCl at pH 8. The DHX−MS spectra monitored as a function of the time of exchange for the destabilized mutant variants have been compared to that of the wt protein (top). The vertical lines in all panels indicate the $m/z$ values for the N state (at 5 s), at the end of each kinetic phase, and for the U state.

**Effect of Destabilization on HX Kinetics of MNEI.** The mass distribution at 5 s of exchange corresponds to that of the N state; 44 ± 1 backbone amide sites could be monitored for the wt as well as the mutant variants in this study. These backbone amide hydrogens served as structural probes, as all other sites exchanged too rapidly to be measured. The mass distribution at the final time point of exchange corresponded to the U state in which 5 ± 1 backbone amide sites remain unexchanged. Because unimodal mass spectra were observed for the wt protein at all exchange times, the deuterium retention was determined from the centroid of the mass distributions, as a function of time



DOI: 10.1021/acs.biochem.7b00367
Biochemistry 2017, 56, 4053−4063

**Table 1. Comparison of the HX Rates and Amplitudes of Mutant Variants of MNEI[a]**

| protein | phase 1 (fast) rate constant ($\times10^{-2}$ $s^{-1}$) | no. of D | phase 2 (slow) rate constant ($\times10^{-4}$ $s^{-1}$) | no. of D | phase 3 (second slow) rate constant ($\times10^{-5}$ $s^{-1}$) | no. of D | phase 4 (very slow) rate constant ($\times10^{-6}$ $s^{-1}$) | no. of D | size of the cooperative unit |
|---|---|---|---|---|---|---|---|---|---|
| wt[b] (0 M GdnHCl) | 1 ± 0.5 | 13 | 3 ± 0.2 | 12 | – | – | 1.4 ± 0.01 | 14 | 0 |
| C42A (pseudo-wt) (0 M GdnHCl) | 0.38 ± 0.6 | 10 | 1.4 ± 0.4 | 12 | – | – | 2.16 ± 0.2 | 11 | 0 |
| A74C (0 M GdnHCl) | 0.98 ± 0.02 | 13 | 1.05 ± 0.01 | 12 | – | – | 1.44 ± 0.08 | 11 | 0 |
| A20C (0 M GdnHCl) | 2.2 ± 0.35 | 11 | 4.7 ± 1.1 | 14 | 6.6 ± 2.9 | 9 | 0.7 ± 0.1 | 6 | 6 |
| L63C (0 M GdnHCl) | 3.25 ± 0.3 | 10 | 4.15 ± 0.35 | 12 | 1.6 ± 0.04 | 10 | 3.85 ± 1.5 | 6 | 6 |
| F90C (0 M GdnHCl) | 2.7 ± 0.4 | 13 | 5.2 ± 1.5 | 14 | 2.1 ± 1.3 | 7 | 2.5 ± 0.7 | 7 | 7 |
| L33A (0 M GdnHCl) | 1.8 ± 0.14 | 10 | 7.8 ± 3.1 | 14 | 1.7 ± 0.1 | 7 | 3.1 ± 1.97 | 8 | 8 |
| wt[b] (1 M GdnHCl) | 1 ± 0.5 | 13 | 3 ± 0.2 | 12 | – | – | 36 ± 8 | 14 | 14 |
| C42A (pseudo-wt) (1 M GdnHCl) | 0.75 ± 0.35 | 12 | 0.95 ± 0.32 | 13 | – | – | 9.55 ± 0.35 | 13 | 13 |
| A20C (1 M GdnHCl) | 1.6 ± 0.2 | 14 | 1.4 ± 0.5 | 13 | | | 130 ± 30 | 14 | 14 |

[a]Note that each mutant variant contained the C42A mutation (see the text), in addition to the mutation specified in its name. Hence, C42A MNEI is the pseudo-wt variant, to which the other mutant variants should be compared. Errors represent the spread in the measurements from two separate experiments. [b]Values taken from ref 31.

(Figure S2). In the case of the destabilized mutant variants, the change in the number of deuteriums that exchange in a noncooperative manner, with respect to time, was quantified from the centroid of the N state distribution, which shifted along the $m/z$ scale with exchange time (Figure 3 and Figure S3). The increase in area under the U state peak with exchange time yielded the apparent rate constant of formation of the U state, which involves the concerted exchange of approximately seven backbone amide sites. The rate constants and corresponding amplitudes obtained from the HX kinetic traces are reported in Table 1. As shown previously for the wt protein,[31] exchange occurred in three distinct kinetic phases: fast, slow, and very slow. In addition to the mass distributions, the exchange kinetics for A74C MNEI was also very similar to that of the wt protein (Figure S2), indicating that in the absence of any change in the global stability of MNEI, HX kinetics remains unperturbed.

For the destabilized mutant variants, A20C, L63C, F90C, and L33A MNEI (Figure 4 and Figure S3), the HX kinetics were significantly different from that of the wt protein. The shift in the centroid of the N state distribution could be fit well only to a sum of three exponentials, while the increase in the area under the U state distribution fit to a single-exponential equation. Hence, unlike for the wt protein and A74C MNEI, the HX kinetics of all the destabilized variants could be described well by invoking only four kinetic phases. Because the HX kinetics of the pseudo-wt protein was similar to that of wt MNEI (Figure S2 and Table 1), the differences observed for the destabilized variants could be attributed entirely to the destabilizing mutations. As reported in Table 1, the rate constants of three of the phases were comparable to those of the wt protein. The additional phase observed for the destabilized variants, with a rate constant on the order of $10^{-5}$ $s^{-1}$, has been called a second slow phase, as it has a rate constant that is intermediate between those of the slow and very slow phases of exchange for the wt protein. The numbers of backbone amide sites that exchanged in the fast and slow phases were similar for the destabilized variants and wt MNEI. In the case of wt MNEI, the 14 remaining sites exchanged in the very slow phase; for all the destabilized mutant variants, ~7−10 sites exchanged in the second slow phase, and the remaining 7 ± 1 sites exchanged in the very slow phase of HX. Moreover, the significantly fewer backbone amide sites that exchanged in the very slow phase for the destabilized mutant variants, compared to the number for the wt protein, opened in a correlated manner resulting in bimodal mass distributions (Figure 3 and Figure S3).

**Identification of the Cooperative Unit in the Mutant Variants.** The locations of the approximately seven backbone amide hydrogens, which exchanged cooperatively in the destabilized mutant variants, were determined by analyzing the HX patterns of individual sequence segments of the protein. The fragments generated by ETD (Figure S1A) were used to determine the extent of exchange in sequence segments of the protein spanning each secondary structural element (Figure S1B,C), as discussed in SI Methods in the Supporting Information.[32]

For each mutant variant, the mass distributions corresponding to all c and z ions, except the c81 (Met1−Thr82) and z78 (Asp22−Pro97) ions, remained unimodal at all times of exchange. The constant widths of the unimodal distributions (Figure 5 and Figures S4−S6) further confirmed that all the observed backbone amide sites in these sequence segments of the protein exchanged in an uncorrelated manner. The observation of bimodality for the Met1−Thr82 (c81 ion) and Asp22−Pro97 (z78 ion) fragments, but not the Ser68−Pro97 (z32 ion) and Met1−Arg40 (c39 ion) fragments, indicated that cooperative exchange of multiple backbone amide sites in a concerted manner was localized to the Pro41−Ala67 sequence segment. Furthermore, the difference in mass between the two peaks observed in the bimodal distributions of the c81 and z78 ions (Figure 5 and Figures S4−S6) corresponded to the cooperative exchange of 7 ± 1 backbone amide sites in each of the mutant variants. This suggested that all the backbone amide sites that exchanged cooperatively upon destabilization of the wt protein were localized to the $\beta2$−$\beta3$ secondary structural elements, spanning the Pro41−Ala67 sequence segment.

**Combined Effect of the Addition of a Denaturant and a Destabilizing Mutation.** The HX−MS results reported so far were obtained by allowing HX to occur at the backbone amide sites of mutant variants of MNEI in the absence of any denaturant, under native conditions. Previously, it had been shown that the addition of the denaturant GdnHCl induced 14 backbone amide sites to exchange cooperatively in wt MNEI.[31,32] In the study presented here, HX−MS kinetics was measured in the presence of a denaturant for the destabilized variant A20C MNEI and compared to the HX kinetics of the wt protein under identical conditions. A20C MNEI was observed to be 0.7 kcal



DOI: 10.1021/acs.biochem.7b00367
Biochemistry 2017, 56, 4053−4063

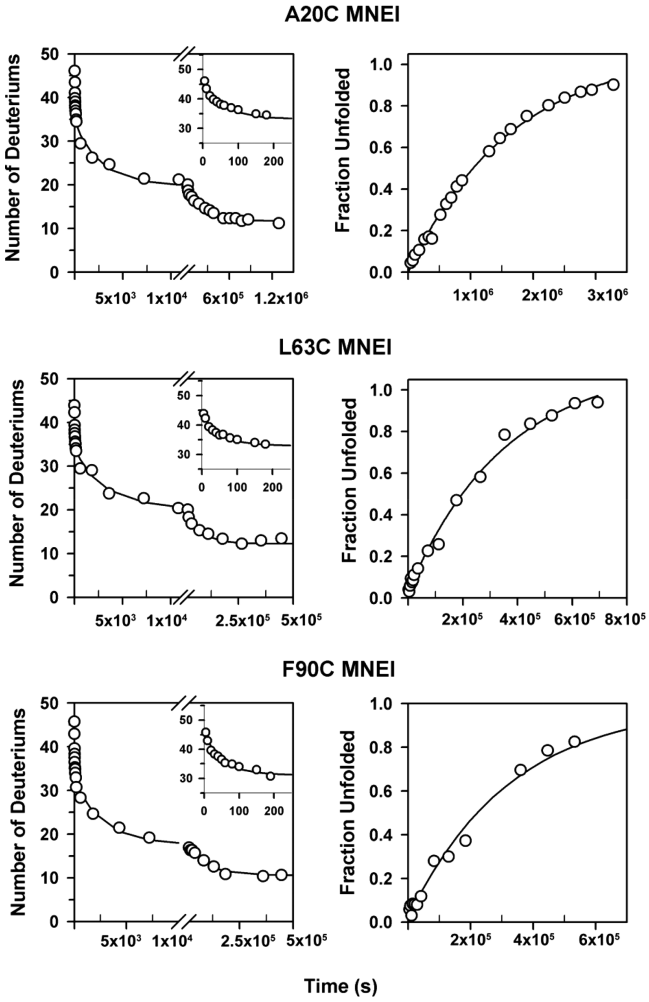


**Figure 4.** DHX−MS kinetics of destabilized variants of MNEI, in 0 M GdnHCl at pH 8. The shift in the centroid $m/z$ value of the higher mass distribution was used to determine the change in deuterium retention with respect to time of exchange (left panels). The increase in the area under the lower mass distribution, which corresponds to the U state, was used to determine the increase in the fraction unfolded, with time (right panels). The solid lines through the data are fits to triple-exponential equations (left panels), or to a single-exponential equation (right panels). The corresponding rate constants and amplitudes are listed in Table 1.

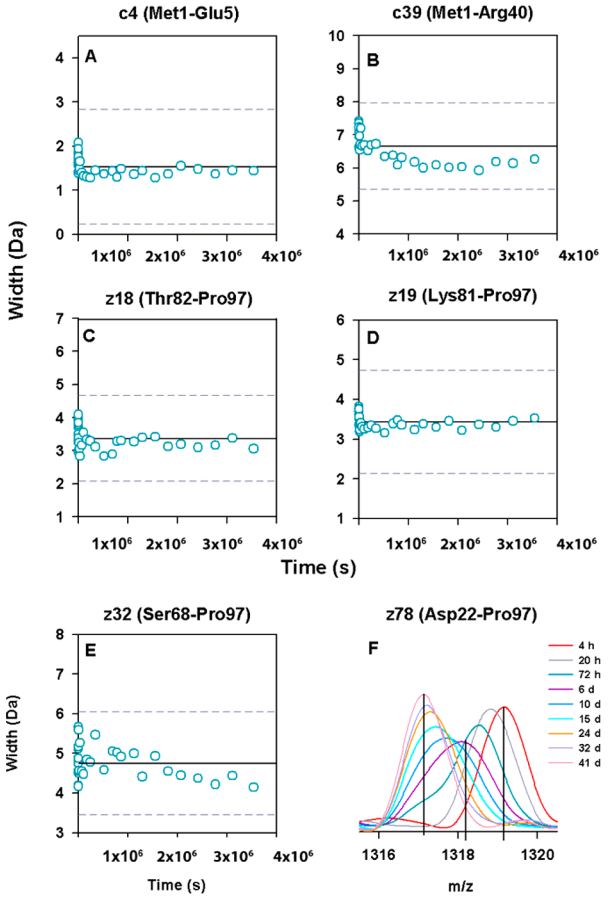


**Figure 5.** Analysis of individual fragments of A20C MNEI subsequent to DHX in 0 M GdnHCl at pH 8. (A−E) The width of the mass distribution (full width at half-maximum), for individual c and z ETD fragment ions of the protein, has been plotted with respect to the time of exchange. In each panel, the solid black line represents the mean width of the mass distribution, and the dashed gray lines correspond to values of the mean width ± 1.3 Da. These limits provide a measure of the maximal widening expected due to stochastic exchange and have been deduced from ref 60. (F) The mass distributions of the z78 (Asp22−Pro97) ion are bimodal for exchange in 0 M GdnHCl for times between 72 h and 41 days. The vertical lines indicate the $m/z$ values at the end of the slow and second slow kinetic phases, and for the U state. The difference in $m/z$ between the centroids of the two mass distributions indicates that seven backbone amide sites exchanged cooperatively.

mol$^{-1}$ less stable than the wt protein. The addition of 1 M GdnHCl caused it to be further destabilized by 3 kcal mol$^{-1}$. As shown in Figure 6, while bimodal distributions were observed for A20C MNEI in 0 M GdnHCl itself, the addition of 1 M GdnHCl resulted in an increase in the separation between the two mass distributions, indicating that a larger number of sites exchanged cooperatively in the presence, than in the absence, of the denaturant. From the centroids of the two peaks observed in the bimodal distribution, it was determined that 14 backbone amide sites exchanged in a correlated manner in A20C MNEI in the presence of 1 M GdnHCl.

Under native conditions, mutational destabilization by 0.7 kcal mol$^{-1}$ (in A20C MNEI) resulted in 32 backbone amide sites exchanging noncooperatively in three kinetic phases, and the seven remaining sites exchanging cooperatively in the very slow phase (Figure 4 and Table 1). In the presence of 1 M GdnHCl, HX into A20C MNEI occurred in three kinetic phases (Figure S7), which agreed well with the HX kinetics observed for the wt protein under identical experimental conditions (Table 1): 27 backbone amide sites in the destabilized variant exchanged noncooperatively in two kinetic phases, while the 14 remaining sites exchanged cooperatively in the very slow phase. As in the case of the wt protein, an analysis of the HX kinetics of individual fragments of A20C MNEI in the presence of 1 M GdnHCl revealed that the 14 cooperatively exchanging backbone amide sites were localized to the $\beta2-\beta3$ segment of the protein (Figure S8).

The HX kinetics of C42A MNEI was also measured in 1 M GdnHCl, a condition in which its stability is equal to that of F90C MNEI in 0 M GdnHCl (3.8 kcal/mol). The resulting mass distributions (Figure S9) were similar to those of wt MNEI in 1 M GdnHCl[31] and indicated that, like in the wt protein, 14 backbone amide sites in the pseudo-wt protein exchanged cooperatively in the presence of a denaturant. The rate constants and amplitudes of the three kinetic phases of exchange are listed in Table 1.



DOI: 10.1021/acs.biochem.7b00367
*Biochemistry* 2017, 56, 4053−4063

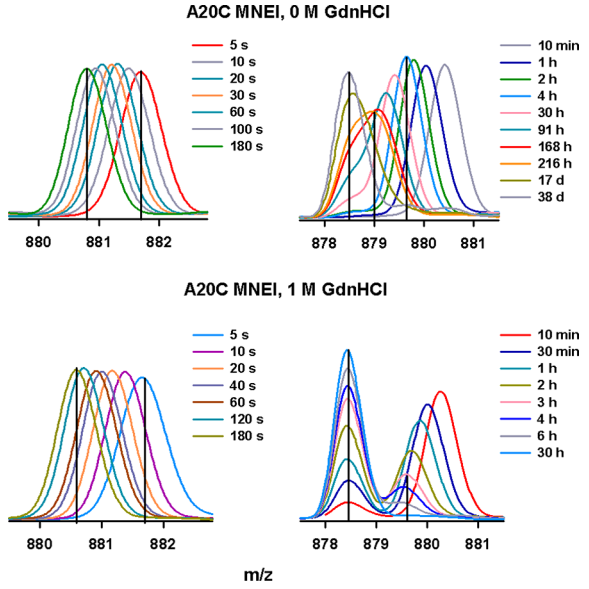


**Figure 6.** Effect of the addition of a denaturant to the destabilized variant A20C MNEI. The mass distributions monitored by DHX−MS have been shown for A20C MNEI in 0 M GdnHCl (top) and in 1 M GdnHCl (bottom). The vertical lines in each panel indicate the $m/z$ values for the N state (at 5 s), at the end of each kinetic phase, and for the U state.

## DISCUSSION

Small barriers and shallow local minima make the free energy landscape of folding of a protein rugged, therefore necessitating the use of a probe that can detect small populations formed as a result of transient sampling, to delineate the landscape roughness. Most spectroscopic probes are sensitive only to larger ensembles of different conformations, the formation of which involves the crossing of major free energy barriers, making it experimentally challenging to delineate ruggedness on the free energy landscape of protein folding and unfolding. In this respect, HX is a powerful methodology that can detect very small populations of intermediate states even in the presence of a large population of the native conformation.[39] Moreover, in conjunction with mass spectrometry, HX experiments provide a measure of the population distributions of the multiple states sampled by the protein, thus delineating the cooperativity of the transition directly.[31,36,40] In the HX−MS study presented here, changes in the kinetic cooperativity of unfolding of MNEI, in response to destabilizing mutations as well as to the addition of a chemical denaturant, have been used to understand the ruggedness inherent to the free energy landscape of folding of this protein.

**Selective Destabilization of the N State Induces Cooperativity in MNEI.** Amino acid mutations might affect both the N and U states of a protein. Nevertheless, similar $m$ values for all the destabilized variants, except L33A MNEI (Table S1), indicated that the U state is largely unperturbed by the mutations made in the study presented here. A change in the $m$ value reflects a change in the surface area exposure of the protein structure upon it undergoing the transition from the N state to the U state[41−43] and is usually interpreted as a change in the degree of structure retained in the U state of the protein.[42−44] The significantly higher $m$ value observed in the case of L33A MNEI (Table S1), therefore, suggests that this mutation may have perturbed the U state, as well. This should be taken into consideration while interpreting the HX kinetics of this protein.

Unimodal mass distributions in the EX1 limit are indicative of noncooperative (uncorrelated) opening transitions preceding the exchange reaction (see the text in the Supporting Information). The unimodal distributions, observed at all times of exchange for wt MNEI under native conditions, therefore indicated that local openings at backbone amide sites, in each kinetic phase, resulted in gradual and noncooperative interconversions between discrete structural intermediates and the globally unfolded state.[31,32] The wide dispersion in the rate constants corresponding to each kinetic phase of HX (Table 1) further indicated the presence of three distinct classes of backbone amide sites with characteristic waiting times for exchange. Because exchange into MNEI under the experimental conditions described here was found to be in the EX1 limit, these opening motions, although local, were unlikely to be local fluctuations and/or breathing motions that are identified typically in the EX2 limit of exchange.[3] Local changes that expose very little surface area have been shown to be associated with structural transitions in a protein.[45] Moreover, the noncooperative loss of structure occurred in a diffuse manner, with backbone amide sites in all parts of MNEI opening in all kinetic phases.[32] The lack of a distinct structural unit observed for MNEI is in stark contrast to the foldon architecture of proteins suggested in previous studies.[3,46,47] The hierarchical sequence of structure-opening events, evident form the dispersion in the HX rates, involves a series of local opening events at one backbone amide site at a time, and not the unfolding of distinct cooperative structural units. Deviations from a hierarchical foldon model[48] for unfolding have been observed for other proteins, as well.[49−52]

The bimodal mass distributions observed only in the case of the destabilized mutant variants (Figure 3 and Figure S3), but not for the wt, pseudo-wt, or A74C MNEI (which is as stable as the wt protein) (Figure S2), indicated that $7 \pm 1$ backbone amide sites were indeed induced to exchange in a concerted manner, under native conditions, by selective destabilization of the N state.

**Destabilized Mutant Variants Exchange in Four Kinetic Phases.** The uncorrelated nature of exchange of the backbone amide sites in wt MNEI, under native conditions, seemed to suggest that the opening motions were driven by random local fluctuations, and not by distinct structure-opening events, of significant amplitude. However, the observation of three distinct kinetic phases for the wt protein (Table 1)[31] suggested that there were multiple waiting times associated with the noncooperative exchange of the backbone amide sites.[31,32] The slow rate constants for exchange of the observed backbone amide sites, several of which are deeply buried in the core of the protein, further indicated that the opening motions in MNEI, although localized to one or two backbone amide sites opening at a time, correspond to structural transitions and not to rapid fluctuations and/or breathing in the N state. Moreover, rapidly fluctuating residues would be expected to exchange in the EX2 limit. Hence, the observation of EX1 exchange for the majority of backbone amide sites[32] provided further evidence that structure-opening events led to exchange under native conditions. The multiple phases of structural opening were characterized in detail for the wt protein in previous studies.[31,32] The fast and slow phases were attributed to the transient formation of two exchange-competent intermediate species, $I_1$ and $I_2$, respectively, while the very slow phase was attributed to the transient formation of the U state.

In contrast to the three kinetic phases of HX observed for wt MNEI, the destabilized mutant variants undergo exchange at backbone amide sites in four kinetic phases (Figure 4 and Figure



DOI: 10.1021/acs.biochem.7b00367
Biochemistry 2017, 56, 4053−4063

S3). An increase in the number of kinetic phases implies an increase in the number of discrete steps involved in the transition, possibly because of the stabilization of intermediate structures, which would in turn indicate a decrease in the cooperativity of the transition between the N and U states, in the destabilized mutant variants, compared to the wt protein. However, the bimodality observed in the mass distributions of the mutant variants (Figure 3 and Figure S2) provides strong evidence of correlated exchange at multiple backbone amide sites, and therefore of an increase in cooperativity, in the destabilized variants, compared to that in wt MNEI. The two observations thus appear to contradict each other.

A previous study[32] that investigated the structural basis of noncooperativity and distinct kinetic phases of opening in wt MNEI revealed a strong coupling between tertiary and secondary interactions in the protein. The discrete kinetic phases could be attributed to the waiting times for the dissolution of individual tertiary packing interactions in MNEI, before the vicinal backbone hydrogen bonding network dissolved. In the study presented here, a longer side chain was replaced by a shorter side chain in the case of L63C, F90C, and L33A MNEI, which is likely to have created a cavity in the protein. The creation of a cavity in the structural core of a protein reduces the stability of the N state[53−57] by weakening the hydrophobic driving force of folding and disrupting packing interactions. Most of the amino acid substitutions investigated in this study are therefore likely to have perturbed tertiary packing interactions in MNEI. Because tertiary and secondary interactions in MNEI are strongly coupled to each other,[32] perturbation of the tertiary packing interactions may manifest as changes in the kinetic phases observed for the dissolution of secondary structure in HX−MS experiments.

The results of this study further highlight the drawbacks of drawing inferences about the cooperativity of protein folding−unfolding transitions from the observed kinetics alone. Although the multiexponential kinetics of the destabilized mutant variants suggests a reduction in cooperativity compared to that of the wt protein, the overall unfolding transition becomes more cooperative upon destabilization of the N state, as inferred directly from the observed population distributions. Hence, an increase in the number of exponentials in a kinetic reaction should not always to be attributed to a decrease in the cooperativity of the transition via stabilization of intermediate structures.

**Smoothing Effect of a Denaturant Inferred from Changes in Cooperativity.** Segmentwise analysis of the HX−MS patterns of wt MNEI and the destabilized mutant variants, in the presence and absence of a denaturant, has shown that the cooperative unfolding unit in this protein is localized to the $\beta2-\beta3$ segment, spanning residues Pro41−Ala67. Under native conditions, all backbone amide sites in the $\beta2-\beta3$ segment of the wt protein opened in an uncorrelated manner in three kinetic phases: fast, slow, and very slow. The destabilization of the N state resulted in cooperative exchange at $7 \pm 1$ backbone amide sites in this segment of the protein, while the addition of GdnHCl to either the wt protein[31,32] or a destabilized mutant variant (Figure 5 and Figures S4−S6) resulted in cooperative exchange at all the observable backbone amide sites (14 in all) in this segment of the protein, as shown in Figure 7.

Although the increase in cooperativity observed upon mutational destabilization as well as addition of denaturant appeared to be due to a change in the stabilities of the N and U states, an interesting result suggested that GdnHCl may also have had other additional effects. The concerted opening of all the backbone amide sites in the $\beta2-\beta3$ segment in a single very slow phase, in the presence of a denaturant, meant that for 25% of the observed sites in this segment, which previously opened in the faster kinetic phases, exchange had been slowed by 3 orders of magnitude in the presence of a denaturant.[31,32] The unusual observation of a decrease in opening rate constants upon addition of GdnHCl, which is expected to promote structure-opening events, suggested the possibility that the denaturant smoothens the free energy barriers associated with the fast and slow phases of exchange of the backbone amide sites in the $\beta2-\beta3$ segment.[32] The results of this study with the destabilized mutant variants confirm the smoothing effect of the denaturant by showing that changes in stability account for cooperative exchange at only 50% of the backbone amide sites in the $\beta2-\beta3$ segment. Cooperative exchange at the remaining 50% sites, observed only in the presence of GdnHCl, can therefore be attributed to the smoothing effect of the chemical denaturant.

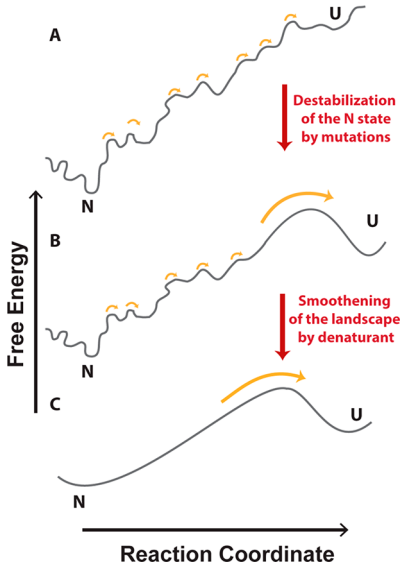


**Figure 7.** Effects of changes in stability, as well as the smoothing of the landscape by the denaturant, on the cooperativity of unfolding of the $\beta2-\beta3$ segment of MNEI. The unfolding of the $\beta2-\beta3$ segment has been shown for (A) wt MNEI in 0 M GdnHCl, (B) the destabilized mutant variants in 0 M GdnHCl, and (C) wt/destabilized mutant variants in 1 M GdnHCl. The small orange arrows correspond to the crossing of marginal barriers, of the order of thermal energy, on a rough free energy landscape of folding, while the large orange arrow corresponds to the crossing of a significant activation free energy barrier. The (un)folding of the remaining structural elements in MNEI remained unperturbed.

The size of the cooperative unit (i.e., the number of backbone amide sites that exchanged in a correlated manner) did not depend upon the extent of destabilization of MNEI. A similar number of sites were observed to exchange cooperatively for A20C MNEI, which was destabilized by only 0.7 kcal $mol^{-1}$, and for F90C MNEI, which was destabilized by 2.5 kcal $mol^{-1}$ (Table 1 and Table S1). A similar result was also observed for the wt protein upon the addition of the denaturant,[31] for which 14 deuteriums exchanged cooperatively in the presence of as little as 0.5 M GdnHCl and as much as 3 M GdnHCl. To further confirm the inference of smoothing of the landscape by GdnHCl, HX was measured under conditions of isostability. It was important to use the pseudo-wt protein (C42A MNEI) for comparison, in this case, to ensure that the increase in the stability of C42A MNEI compared to that of the wt protein did not affect the results.


DOI: 10.1021/acs.biochem.7b00367
Biochemistry 2017, 56, 4053−4063

C42A MNEI in 1 M GdnHCl and F90C MNEI in 0 M GdnHCl have the same stability (3.8 kcal/mol). However, while the former underwent cooperative exchange at 14 backbone amide sites (Figure S9), the latter exchanged at only seven sites cooperatively. These observations provide strong evidence of the smoothing effect of the denaturant.

A segmentwise analysis of the HX−MS patterns of the wt[32] and the mutant variants further established that the extent of cooperativity induced in MNEI, upon destabilization of the N state via mutations, also did not show any correlation to the structural location of the mutated residue. The amino acid residues mutated in this study were present not only in $\beta$2 and $\beta$3, which constitute the cooperative unit in MNEI in the presence of the denaturant,[31] but also in the helix and in a loop region (Figure 2). The observation that the size and the location of the cooperative unit were the same for all the mutant variants, which were destabilized to different extents, suggests that these site-specific mutations affect the stability of MNEI in a global manner, as do denaturants.

**Ruggedness on the Free Energy Landscape of Protein Folding.** A previous study of a downhill folding protein inferred a similar smoothing effect of the denaturant on the free energy landscape of protein folding.[18] The addition of small amounts of GdnHCl, which is expected to increase the activation energy barrier to folding by preferential stabilization of the U state, resulted in an increase in the activated time scale, corresponding to the crossing of the activation free energy barrier. Interestingly, however, the presence of the denaturant also shortened the molecular time scale, corresponding to the relaxation of molecules from the top of the activation energy barrier to the native well. This indicated that the denaturant smoothened the roughness caused by small free energy barriers and shallow local minima, thereby increasing the speed of the downhill folding reaction.[17,18] In the case of (un)folding transitions limited by one large energy barrier or a few of them, the population of intermediate conformations separated by small ($<3\ k_BT$) barriers, which contribute to the roughness of the free energy landscape, may be either misfolded or productive species. Although a decrease in the size of the population of misfolded species, which serve as kinetic traps and slow folding, would increase the folding rate, smoothing may also result in a decrease in the level of obligatory intermediates that are productive for the folding reaction.[6] The interpretation of the effects of smoothing of a rugged free energy surface is, therefore, not simple for a barrier-limited reaction. The effect of a decrease in ruggedness in such cases depends on what role the intermediates play in the folding−unfolding transition.

The most obvious way in which denaturants may smoothen the free energy landscape of folding is by perturbing the stabilities, and thereby reducing the size of the population, of intermediate structures.[48] It is, however, also possible that protein molecules are preferentially channelled along specific routes on the free energy landscape in the presence of the denaturant. The smoothing observed upon the addition of GdnHCl may, therefore, reflect differences in ruggedness along the different pathways on the free energy landscape. This effect of the denaturant would therefore be akin to the effect of chaperones,[58] mutational changes as well as changes in temperature that have been shown to modulate ruggedness by restricting the landscape that is accessible to the protein for folding.[59]

## CONCLUSION

In the study presented here, HX−MS experiments in the EX1 limit have been used to monitor changes in the kinetic cooperativity of the unfolding of MNEI under native conditions. The changes in cooperativity in response to selective destabilization of the N state, as well as to the addition of denaturant, have been used to directly delineate the smoothing of a rough free energy landscape of folding. Amino acid mutations that destabilized the N state selectively caused a subset of seven backbone amide sites, in the slowly exchanging core of MNEI, to open cooperatively in the very slow phase, under native conditions. In contrast, the entire backbone hydrogen bonding network in wt MNEI opened gradually, under identical conditions. A lack of correlation of the size of the cooperative unit with the extent of destabilization of the N state, or with the location of the destabilizing residue, further indicated that the cooperative unit is inherent to the structure of MNEI and cannot be modulated by changing only stability, to include more elements of secondary structure. Only upon the addition of the denaturant was there an increase in the number of backbone amide sites that exchanged cooperatively; seven additional sites opened in a concerted manner, in all the destabilized variants. Segmentwise analysis of the HX kinetics of the destabilized mutant variants in the presence and absence of the denaturant further showed that the increased cooperativity could be attributed to the smoothing of the rough free energy surface of MNEI.

## ASSOCIATED CONTENT

### Supporting Information

The Supporting Information is available free of charge on the ACS Publications website at DOI: 10.1021/acs.biochem.7b00367.

SI Methods, SI Text, Table S1, and Figures S1−S8 (PDF)

## AUTHOR INFORMATION


### Corresponding Author

*Fax: 91-80-23636662. E-mail: jayant@ncbs.res.in.

### ORCID

Pooja Malhotra: 0000-0003-1871-8259

Prashant N. Jethva: 0000-0002-7704-2810

Jayant B. Udgaonkar: 0000-0002-7005-224X



### Funding

J.B.U. is a recipient of a J. C. Bose National Research Fellowship from the Government of India. This work was funded by the Tata Institute of Fundamental Research and by the Department of Science and Technology, Government of India.

### Notes

The authors declare no competing financial interest.

## ACKNOWLEDGMENTS

We thank the members of our laboratory for discussions.


## ABBREVIATIONS

MNEI, single-chain monellin; GdnHCl, guanidine hydrochloride; HX−MS, hydrogen exchange coupled to mass spectrometry; ETD, electron transfer dissociation.

## REFERENCES


(1) McCammon, J. A., Gelin, B. R., and Karplus, M. (1977) Dynamics of folded proteins. *Nature 267*, 585−590.




DOI: 10.1021/acs.biochem.7b00367
*Biochemistry* 2017, 56, 4053−4063

(2) Henzler-Wildman, K., and Kern, D. (2007) Dynamic personalities of proteins. *Nature 450*, 964−972.
(3) Bai, Y., Sosnick, T. R., Mayne, L., and Englander, S. W. (1995) Protein folding intermediates: native-state hydrogen exchange. *Science 269*, 192−197.
(4) Rami, B. R., and Udgaonkar, J. B. (2002) Mechanism of Formation of a Productive Molten Globule Form of Barstar. *Biochemistry 41*, 1710−1716.
(5) Cecconi, C., Shank, E. A., Bustamante, C., and Marqusee, S. (2005) Direct Observation of the Three-State Folding of a Single Protein Molecule. *Science 309*, 2057−2060.
(6) Ellison, P. A., and Cavagnero, S. (2006) Role of unfolded state heterogeneity and en-route ruggedness in protein folding kinetics. *Protein Sci. 15*, 564−582.
(7) Malhotra, P., and Udgaonkar, J. B. (2014) High-Energy Intermediates in Protein Unfolding Characterized by Thiol Labeling under Nativelike Conditions. *Biochemistry 53*, 3608−3620.
(8) Jahn, T. R., and Radford, S. E. (2005) The Yin and Yang of protein folding. *FEBS J. 272*, 5962−5970.
(9) Bollen, Y. J. M., Kamphuis, M. B., and van Mierlo, C. P. M. (2006) The folding energy landscape of apoflavodoxin is rugged: Hydrogen exchange reveals nonproductive misfolded intermediates. *Proc. Natl. Acad. Sci. U. S. A. 103*, 4095−4100.
(10) Chiti, F., and Dobson, C. M. (2009) Amyloid formation by globular proteins under native conditions. *Nat. Chem. Biol. 5*, 15−22.
(11) Go, N. (1983) Theoretical Studies of Protein Folding. *Annu. Rev. Biophys. Bioeng. 12*, 183−210.
(12) Sosnick, T. R., Mayne, L., Hiller, R., and Englander, S. W. (1994) The barriers in protein folding. *Nat. Struct. Biol. 1*, 149−156.
(13) Bryngelson, J. D., Onuchic, J. N., Socci, N. D., and Wolynes, P. G. (1995) Funnels, pathways, and the energy landscape of protein folding: A synthesis. *Proteins: Struct., Funct., Genet. 21*, 167−195.
(14) Chan, H. S., Zhang, Z., Wallin, S., and Liu, Z. (2011) Cooperativity, Local-Nonlocal Coupling, and Nonnative Interactions: Principles of Protein Folding from Coarse-Grained Models. *Annu. Rev. Phys. Chem. 62*, 301.
(15) Sabelko, J., Ervin, J., and Gruebele, M. (1999) Observation of strange kinetics in protein folding. *Proc. Natl. Acad. Sci. U. S. A. 96*, 6031−6036.
(16) Garcia-Mira, M. M., Sadqi, M., Fischer, N., Sanchez-Ruiz, J. M., and Muñoz, V. (2002) Experimental Identification of Downhill Protein Folding. *Science 298*, 2191−2195.
(17) Yang, W. Y., and Gruebele, M. (2003) Folding at the speed limit. *Nature 423*, 193−197.
(18) Yang, W. Y., and Gruebele, M. (2004) Folding lambda-repressor at its speed limit. *Biophys. J. 87*, 596−608.
(19) Yang, W. Y., Pitera, J. W., Swope, W. C., and Gruebele, M. (2004) Heterogeneous Folding of the trpzip Hairpin: Full Atom Simulation and Experiment. *J. Mol. Biol. 336*, 241−251.
(20) Gelman, H., and Gruebele, M. (2014) Fast protein folding kinetics. *Q. Rev. Biophys. 47*, 95−142.
(21) Ansari, A., Jones, C. M., Henry, E. R., Hofrichter, J., and Eaton, W. A. (1992) The role of solvent viscosity in the dynamics of protein conformational changes. *Science 256*, 1796−1798.
(22) Plaxco, K. W., and Baker, D. (1998) Limited internal friction in the rate-limiting step of a two-state protein folding reaction. *Proc. Natl. Acad. Sci. U. S. A. 95*, 13591−13596.
(23) Pradeep, L., and Udgaonkar, J. B. (2007) Diffusional Barrier in the Unfolding of a Small Protein. *J. Mol. Biol. 366*, 1016−1028.
(24) Cellmer, T., Henry, E. R., Hofrichter, J., and Eaton, W. A. (2008) Measuring internal friction of an ultrafast-folding protein. *Proc. Natl. Acad. Sci. U. S. A. 105*, 18320−18325.
(25) Wensley, B. G., Batey, S., Bone, F. a C., Chan, Z. M., Tumelty, N. R., Steward, A., Kwa, L. G., Borgia, A., and Clarke, J. (2010) Experimental evidence for a frustrated energy landscape in a three-helix-bundle protein family. *Nature 463*, 685−8.
(26) Soranno, A., Buchli, B., Nettels, D., Cheng, R. R., Müller-Späth, S., Pfeil, S. H., Hoffmann, A., Lipman, E. A., Makarov, D. E., and Schuler, B. (2012) Quantifying internal friction in unfolded and intrinsically disordered proteins with single-molecule spectroscopy. *Proc. Natl. Acad. Sci. U. S. A. 109*, 17800−17806.
(27) Rhoades, E., Cohen, M., Schuler, B., and Haran, G. (2004) Two-State Folding Observed in Individual Protein Molecules. *J. Am. Chem. Soc. 126*, 14686−14687.
(28) Chung, H. S., Piana-Agostinetti, S., Shaw, D. E., and Eaton, W. A. (2015) Structural origin of slow diffusion in protein folding. *Science 349*, 1504−1510.
(29) Neupane, K., Foster, D. A. N., Dee, D. R., Yu, H., Wang, F., and Woodside, M. T. (2016) Direct observation of transition paths during the folding of proteins and nucleic acids. *Science 352*, 239−242.
(30) Gruebele, M. (2008) Comment on probe-dependent and nonexponential relaxation kinetics: Unreliable signatures of downhill protein folding. *Proteins: Struct., Funct., Genet. 70*, 1099−1102.
(31) Malhotra, P., and Udgaonkar, J. B. (2015) Tuning Cooperativity on the Free Energy Landscape of Protein Folding. *Biochemistry 54*, 3431−3441.
(32) Malhotra, P., and Udgaonkar, J. B. (2016) Secondary structural change can occur diffusely and not modularly during protein folding and unfolding reactions. *J. Am. Chem. Soc. 138*, 5866−5878.
(33) Patra, A. K., and Udgaonkar, J. B. (2007) Characterization of the folding and unfolding reactions of single-chain monellin: evidence for multiple intermediates and competing pathways. *Biochemistry 46*, 11727−11743.
(34) Agashe, V. R., and Udgaonkar, J. B. (1995) Thermodynamics of denaturation of barstar: evidence for cold denaturation and evaluation of the interaction with guanidine hydrochloride. *Biochemistry 34*, 3286−99.
(35) Jha, S. K., Dhar, D., Krishnamoorthy, G., and Udgaonkar, J. B. (2009) Continuous dissolution of structure during the unfolding of a small protein. *Proc. Natl. Acad. Sci. U. S. A. 106*, 11113−8.
(36) Ferraro, D. M., Lazo, N. D., and Robertson, A. D. (2004) EX1 Hydrogen Exchange and Protein Folding. *Biochemistry 43*, 587−594.
(37) Bruix, M., Ribó, M., Benito, A., Laurents, D. V., Rico, M., and Vilanova, M. (2008) Destabilizing mutations alter the hydrogen exchange mechanism in ribonuclease A. *Biophys. J. 94*, 2297−305.
(38) Hvidt, A., and Nielsen, S. O. (1966) Hydrogen Exchange in Proteins. *Adv. Protein Chem. 21*, 287−386.
(39) Englander, S. W. (2000) Protein Folding Intermediates and Pathways Studied by Hydrogen Exchange. *Annu. Rev. Biophys. Biomol. Struct. 29*, 213−238.
(40) Malhotra, P., and Udgaonkar, J. B. (2016) How cooperative are protein folding and unfolding transitions? *Protein Sci. 25*, 1924−1941.
(41) Schellman, J. a. (2002) Fifty years of solvent denaturation. *Biophys. Chem. 96*, 91−101.
(42) Shortle, D. (1995) Staphylococcal Nuclease: A Showcase of m-Value Effects. In *Protein Stability* (Anfinsen, C. B., Edsall, J. T., and Eisenberg, D. S., Eds.) Advances in Protein Chemistry, pp 217−247, Academic Press.
(43) Pradeep, L., and Udgaonkar, J. B. (2004) Osmolytes Induce Structure in an Early Intermediate on the Folding Pathway of Barstar. *J. Biol. Chem. 279*, 40303−40313.
(44) Dill, K. A., and Shortle, D. (1991) Denatured States of Proteins. *Annu. Rev. Biochem. 60*, 795−825.
(45) Maity, H., Lim, W. K., Rumbley, J. N., and Englander, S. W. (2003) Protein hydrogen exchange mechanism: Local fluctuations. *Protein Sci. 12*, 153−160.
(46) Fuentes, E. J., and Wand, A. J. (1998) Local Dynamics and Stability of Apocytochrome b 562 Examined by Hydrogen. *Biochemistry 37*, 3687−3698.
(47) Bédard, S., Mayne, L. C., Peterson, R. W., Wand, A. J., and Englander, S. W. (2008) The Foldon Substructure of Staphylococcal Nuclease. *J. Mol. Biol. 376*, 1142−1154.
(48) Englander, S. W. (2000) Protein folding intermediates and pathways studied by protein folding. *Annu. Rev. Biophys. Biomol. Struct. 29*, 213−238.
(49) Arrington, C. B., and Robertson, A. D. (2000) Correlated motions in native proteins from MS analysis of NH exchange: evidence for a manifold of unfolding reactions in ovomucoid third domain. *J. Mol. Biol. 300*, 221−232.


DOI: 10.1021/acs.biochem.7b00367
*Biochemistry* 2017, 56, 4053−4063

(50) Schanda, P., Forge, V., and Brutscher, B. (2007) Protein folding and unfolding studied at atomic resolution by fast two-dimensional NMR spectroscopy. *Proc. Natl. Acad. Sci. U. S. A. 104*, 11257−11262.
(51) Llinas, M., Gillespie, B., Dahlquist, F. W., and Marqusee, S. (1999) The energetics of T4 lysozyme reveal a hierarchy of conformations. *Nat. Struct. Biol. 6*, 1072−1078.
(52) Krishna Mohan, P. M., Chakraborty, S., and Hosur, R. (2009) NMR investigations on residue level unfolding thermodynamics in DLC8 dimer by temperature dependent native state hydrogen exchange. *J. Biomol. NMR 44*, 1−11.
(53) Kellis, J. T., Nyberg, K., Sail, D., and Fersht, A. R. (1988) Contribution of hydrophobic interactions to protein stability. *Nature 333*, 784−786.
(54) Eriksson, A. E., Baase, W. A., Zhang, X. J., Heinz, D. W., Blaber, M., Baldwin, E. P., and Matthews, B. W. (1992) Response of a protein structure to cavity-creating mutations and its relation to the hydrophobic effect. *Science (Washington, DC, U. S.) 255*, 178−183.
(55) Varadarajan, R., and Richards, F. M. (1992) Crystallographic structures of ribonuclease S variants with nonpolar substitution at position 13: packing and cavities. *Biochemistry 31*, 12315−12327.
(56) Buckle, A. M., Henrick, K., and Fersht, A. R. (1993) Crystal Structural Analysis of Mutations in the Hydrophobic Cores of Barnase. *J. Mol. Biol. 234*, 847−860.
(57) Jackson, S. E., Moracci, M., elMasry, N., Johnson, C. M., and Fersht, A. R. (1993) Effect of cavity-creating mutations in the hydrophobic core of chymotrypsin inhibitor 2. *Biochemistry 32*, 11259−11269.
(58) Patra, A. K., and Udgaonkar, J. B. (2009) GroEL can unfold late intermediates populated on the folding pathways of monellin. *J. Mol. Biol. 389*, 759−75.
(59) Nguyen, H., Jager, M., Moretto, A., Gruebele, M., and Kelly, J. W. (2003) Tuning the free-energy landscape of a WW domain by temperature, mutation, and truncation. *Proc. Natl. Acad. Sci. U. S. A. 100*, 3948−53.
(60) Weis, D. D., Wales, T. E., Engen, J. R., Hotchko, M., and Ten Eyck, L. F. (2006) Identification and Characterization of EX1 Kinetics in H/D Exchange Mass Spectrometry by Peak Width Analysis. *J. Am. Soc. Mass Spectrom. 17*, 1498−1509.



DOI: 10.1021/acs.biochem.7b00367
*Biochemistry* 2017, 56, 4053−4063